Sampling from binary measurements - On Reconstructions from Walsh coefficients

Laura Thesing

University of Cambridge – Applied Functional and Harmonic Analysis
joint work with Anders Hansen

28 October 2020

Motivation

Sampling and reconstruction in every day life:

- Surfing the internet
- Taking pictures
- Listening to music

www.clker.com, www.flaticon.com, clipart-library.com

Fluorescence Microscopy

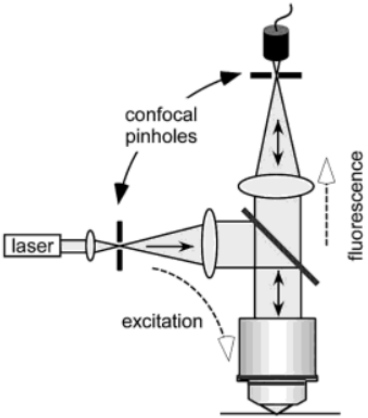

Figure: Schematic representation of fluorescence microscope

Table of content

Spaces

- Sampling space:
  $\mathcal{S} = \overline{\text{span}} \{\omega_k : k \in \mathbb{N}\}$ and $\mathcal{S}_N = \text{span} \{\omega_k : k = 1, \ldots, N\}$
- Linear measurements:
  $m_k = \langle f, \omega_k \rangle, \quad k \in \mathbb{N}$
- Reconstruction space:
  $\mathcal{R} = \overline{\text{span}} \{\varphi_k : k \in \mathbb{N}\}$ and $\mathcal{R}_M = \text{span} \{\varphi_k : k = 1, \ldots, M\}$

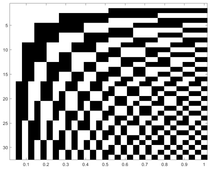

(a) Walsh functions

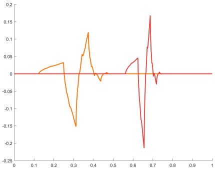

(b) Daubechies 4 wavelet

Figure: Reconstruction and Sampling function

Change of basis matrix

Notation:

$$U = \begin{pmatrix} u_{11} & \dots & u_{1M} & \dots \\ \vdots & \ddots & \vdots & \\ u_{N1} & \dots & u_{NM} & \\ \vdots & & & \ddots \end{pmatrix} \text{ with } u_{ij} = \langle \omega_i, \varphi_j \rangle$$

We denote with

$$U^{[N,M]} = P_N U P_M$$

the part of the matrix of the first N columns and M rows and with

$$\alpha^{[N]} = [\alpha_1, \dots, \alpha_M] \text{ and } m^{[M]} = [m_1, \dots, m_N]^T .$$

Reconstruction Methods

Desired properties:

- Accuracy,
- Stability and
- Sometimes consistency.

Generalized Sampling and the PBDW-method

One calculates the least sqare solution of the following linear equation for $\alpha^{[M]} \in \mathbb{R}^M$:

$$U^{[M,N]}\alpha^{[M]} = m(f)^{[N]},$$

where $m(f)^{[N]} = (m(f)_1, \ldots, m(f)_N) \in \mathbb{R}^N$. The solution is given by

$$G_{N,M}(f) = \sum_{i=1}^{M} \alpha_i \varphi_i.$$

For the PBDW-method the solution is tweaked to be **consistent**, i.e.

$$D_{N,M}(f) = G_{N,M}(f) + P_{\mathcal{S}_N}(f) - P_{\mathcal{S}_N}(G_{N,M}(f)).$$

Generalized Sampling and the PBDW-method

One calculates the least sqare solution of the following linear equation for $\alpha^{[M]} \in \mathbb{R}^M$:

$$U^{[M,N]}\alpha^{[M]} = m(f)^{[N]},$$

where $m(f)^{[N]} = (m(f)_1, \dots, m(f)_N) \in \mathbb{R}^N$. The solution is given by

$$G_{N,M}(f) = \sum_{i=1}^{M} \alpha_i \varphi_i.$$

For the PBDW-method the solution is tweaked to be **consistent**, i.e.

$$D_{N,M}(f) = G_{N,M}(f) + P_{\mathcal{S}_N}(f) - P_{\mathcal{S}_N}(G_{N,M}(f)).$$

Generalized Sampling and the PBDW-method

One calculates the least sqare solution of the following linear equation for $\alpha^{[M]} \in \mathbb{R}^M$:

$$U^{[M,N]}\alpha^{[M]} = m(f)^{[N]},$$

where $m(f)^{[N]} = (m(f)_1, \ldots, m(f)_N) \in \mathbb{R}^N$. The solution is given by

$$G_{N,M}(f) = \sum_{i=1}^{M} \alpha_i \varphi_i.$$

For the PBDW-method the solution is tweaked to be **consistent**, i.e.

$$D_{N,M}(f) = G_{N,M}(f) + P_{\mathcal{S}_N}(f) - P_{\mathcal{S}_N}(G_{N,M}(f)).$$

Subspace Angle

The quality of both methods depends highly on the subspace angle

$$\cos(\omega(\mathcal{R}_M, \mathcal{S}_N)) = \inf_{\varphi \in \mathcal{R}_M, \|\varphi\|=1} \|P_{\mathcal{S}_N}\varphi\| = \frac{1}{\mu(\mathcal{R}_M, \mathcal{S}_N)},$$

The condition number κ for both methods is

$$\kappa(\mathcal{R}_M, \mathcal{S}_N) = \mu(\mathcal{R}_M, \mathcal{S}_N).$$

and they are optimal up to $\mu(\mathcal{R}_M, \mathcal{S}_N)$.

Subspace Angle

The quality of both methods depends highly on the subspace angle

$$\cos(\omega(\mathcal{R}_M, \mathcal{S}_N)) = \inf_{\varphi \in \mathcal{R}_M, \|\varphi\|=1} \|P_{\mathcal{S}_N}\varphi\| = \frac{1}{\mu(\mathcal{R}_M, \mathcal{S}_N)},$$

The condition number κ for both methods is

$$\kappa(\mathcal{R}_M, \mathcal{S}_N) = \mu(\mathcal{R}_M, \mathcal{S}_N).$$

and they are optimal up to $\mu(\mathcal{R}_M, \mathcal{S}_N)$.

Subspace Angle

The quality of both methods depends highly on the subspace angle

$$\cos(\omega(\mathcal{R}_M, \mathcal{S}_N)) = \inf_{\varphi \in \mathcal{R}_M, \|\varphi\|=1} \|P_{\mathcal{S}_N}\varphi\| = \frac{1}{\mu(\mathcal{R}_M, \mathcal{S}_N)},$$

The condition number κ for both methods is

$$\kappa(\mathcal{R}_M, \mathcal{S}_N) = \mu(\mathcal{R}_M, \mathcal{S}_N).$$

and they are optimal up to $\mu(\mathcal{R}_M, \mathcal{S}_N)$.

Non-linear Reconstruction Methods

Use the sparsity of the signal and subsampling ⇒ Compressed sensing

Non-linear Reconstruction Methods

Use the sparsity of the signal and subsampling ⇒ Compressed sensing
Solve ℓ_1 minimization problem:

$$\min_{\alpha \in \ell^1(\mathbb{N})} \|\alpha\|_{\ell^1} \text{ subject to } \|P_\Omega U \alpha - m_\Omega\|_2 \leq \delta,$$

where Ω is the sampling pattern and m_Ω the samples with the index in Ω.

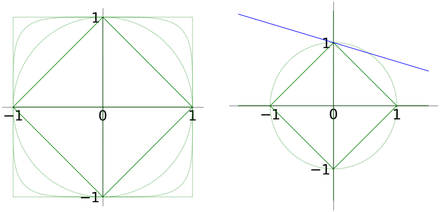

(a) Norm balls (b) Norm balls

Figure: Intuition for norm choices

Classic CS to Structured CS

Classic CS

- Chooses Ω to be fully random
- Does not use the additional structure
- Needs incoherence of the reconstruction matrix

Structured CS

- Takes the special sparsity structure of the signal into account
- Resolves the high coherence in the first elements with more samples in this area and fewer samples later
- Needs to be adapted to application type

Recovery Guarantees

Need to ensure that the reconstruction is **guaranteed**:

- Linear methods: relationship number of samples N to number of coefficients M
  $\rightarrow$ Stable sampling rate (SSR)
- Non-linear methods: Choice of the sampling pattern Ω and the maximal sampling bandwidth N with the balancing property
  $\rightarrow$ Non-uniform recovery guarantees

Walsh functions

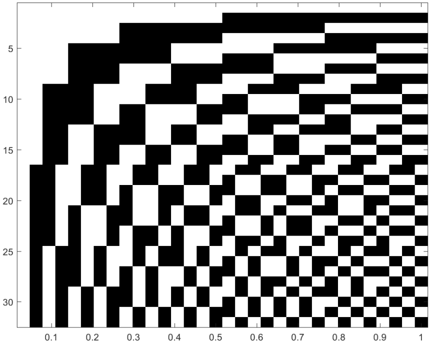

Figure: The first 32 Walsh functions

The generalized Walsh functions in $L^2([0,1])$ are given by

$$\mathrm{Wal}(s,x) = (-1)^{\sum_{i\in\mathbb{Z}}(s_i+s_{i+1})x_{-i-1}}.$$

with $s = \sum_{i\in\mathbb{Z}} s_i 2^{i-1}$ with $s_i \in \{0,1\}$ and $x = \sum_{i\in\mathbb{Z}} x_i 2^{i-1}$ with $x_i \in \{0,1\}$.

Wavelets

For some mother wavelet ψ we get the Wavelet space

$$W = \left\{ \psi_{j,k}(x) = 2^{j/2}\psi(2^j x - k), k = 0, \ldots, 2^j - 1, j \in \mathbb{Z} \right\}.$$

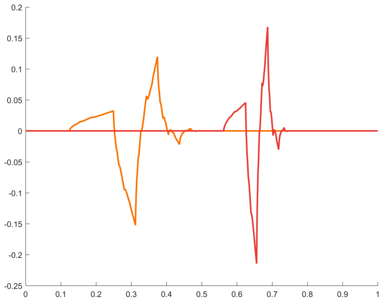

Figure: Daubechies 4 wavelet

Sparsity Structure

Natural data is not only sparse in the representation space but sparse in levels.

- The number of non-zero coefficients decreases in higher levels
- The largest coefficients exist in lower levels
- Large values because of discontinuities repeat themselves in all levels

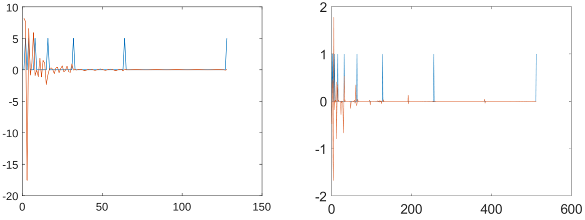

Figure: Sparsity structure for smooth and discontinuous signal

Sparsity Structure

Definition (Adcock et al.)

The set of $(\mathbf{s}, \mathbf{M})$- sparse vectors is $\Sigma_{\mathbf{s},\mathbf{M}}$ with

$$\Delta_k := \operatorname{supp}(x) \cap \{M_{k-1} + 1, \ldots, M_k\},$$

satisfies $|\Delta_k| \leq s_k$ for all $k = 1, \ldots, r$. The approximation error is

$$\sigma_{\mathbf{s},\mathbf{M}}(x) = \min_{\eta \in \Sigma_{\mathbf{s},\mathbf{M}}} \|x - \eta\|_{\ell^1}.$$

Reconstruction Matrix

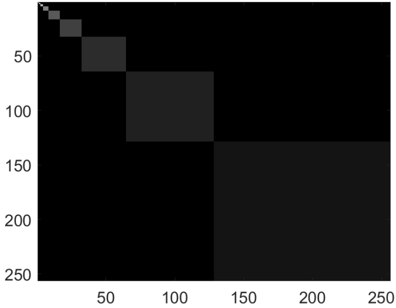

(a) Walsh samples and Haar Wavelets

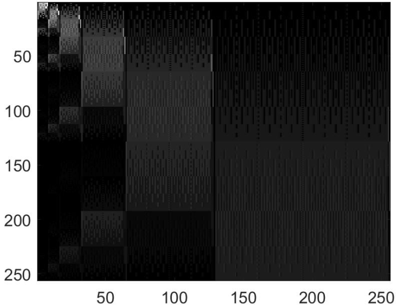

(b) Walsh samples and boundary Wavelets of order 2

Figure: Change of basis matrix U

Intuition

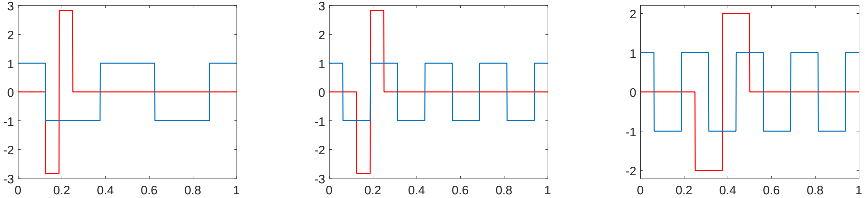

(a) Cancelation by highlevel wavelet

(b) No cancelation

(c) Cancelation by high sequency Walsh function

Figure: Intuition for reconstruction matrix structure

Level structure and the ordering for the sampling bands

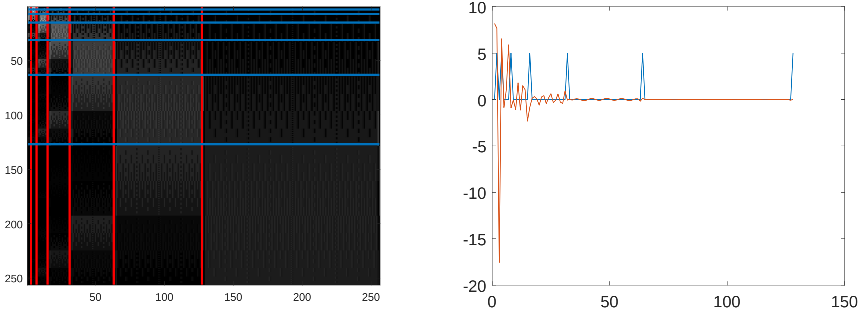

Figure: Reconstruction matrix and potential wavelet coefficients

Multilevel sampling scheme

Definition (Adcock et al.)

The sampling set

$$\Omega = \Omega_{\mathbf{N},\mathbf{m}} = \Omega_1 \cup \ldots \cup \Omega_r.$$

is the MLS with samples chosen at random in each level

$$\Omega_k \subset \{N_{k-1}+1,\ldots,N_k\}, \quad |\Omega_k| = m_k, \quad k = 1,\ldots,r.$$

Linearity of the Stable Sampling Rate

Theorem (Hansen, T.)

Let $M = 2^{dR}$ with some $R \in \mathbb{N}$ the amount of reconstructed coefficients, then there exists for all $\theta \in (1, \infty)$ a constant S_θ such that for all amount of samples with

$$N \geq 2^{dR} S_\theta$$

we have

$$\mu(\mathcal{R}_M, \mathcal{S}_N) \leq \theta.$$

Non-uniform recovery results in 1D

Theorem (Hansen, T.)

Let $\Omega = \Omega_{N,m}$ be a multilevel sampling scheme such that the following holds:

1. $$N \gtrsim M^2 \cdot \log_2(C_1).$$

2. *For each $k = 1, \dots, r$,*

$$m_k \gtrsim \log(\epsilon^{-1}) \log\left(C_2\right) \left(\sum_{l=1}^{r} 2^{-|k-l|/2} s_l\right)$$

Then with probability exceeding $1 - s\epsilon$, any minimizer $\alpha \in \ell^1(\mathbb{N})$ satisfies

$$||\alpha - x||_2 \leq c \cdot \left(\delta(1 + C_3\sqrt{s}) + \sigma_{s,M}(f)\right).$$

Non-uniform recovery results in 1D

Theorem (Hansen, T.)

Let $\Omega = \Omega_{N,m}$ be a multilevel sampling scheme such that the following holds:

1. $$N \gtrsim M^2 \cdot \log_2(C_1).$$
2. *For each* $k = 1, \ldots, r$,

$$m_k \gtrsim \log(\epsilon^{-1}) \log\left(C_2\right) \left(\sum_{l=1}^{r} 2^{-|k-l|/2} s_l \right)$$

Then with probability exceeding $1 - s\epsilon$*, any minimizer* $\alpha \in \ell^1(\mathbb{N})$ *satisfies*

$$\|\alpha - x\|_2 \leq c \cdot \left(\delta(1 + C_3\sqrt{s}) + \sigma_{s,M}(f) \right).$$

Non-uniform recovery results in 1D

Theorem (Hansen, T.)

Let $\Omega = \Omega_{N,m}$ be a multilevel sampling scheme such that the following holds:

1. $$N \gtrsim M^2 \cdot \log_2(C_1).$$
2. *For each $k = 1, \dots, r$,*
$$m_k \gtrsim \log(\epsilon^{-1}) \log\left(C_2\right) \left(\sum_{l=1}^{r} 2^{-|k-l|/2} s_l\right)$$

Then with probability exceeding $1 - s\epsilon$, any minimizer $\alpha \in \ell^1(\mathbb{N})$ satisfies

$$\|\alpha - x\|_2 \leq c \cdot \left(\delta(1 + C_3\sqrt{s}) + \sigma_{s,M}(f)\right).$$

Stable Sampling Rate

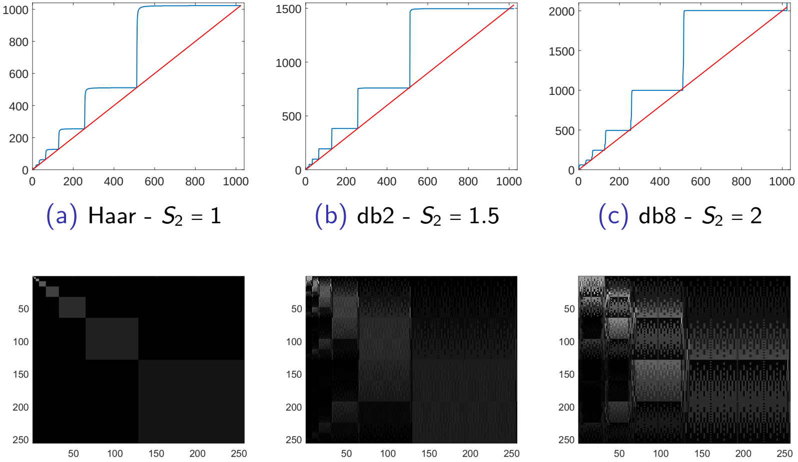

(a) Haar - $S_2 = 1$ (b) db2 - $S_2 = 1.5$ (c) db8 - $S_2 = 2$

(d) Haar-Walsh (e) db2 - Walsh (f) db8 - Walsh

Figure: Stable sampling rate for $\theta = 2$ and reconstruction matrix

Linear Reconstruction

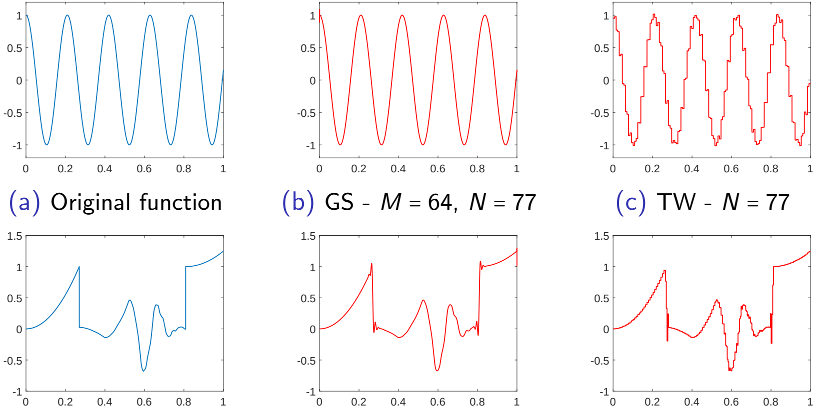

(a) Original function
(b) GS - $M = 64,\ N = 77$
(c) TW - $N = 77$
(d) Original function
(e) GS- $M = 128, N = 192$
(f) TW - $N = 192$

Figure: Reconstruction with Daubechies 8 Wavelets and the inverse Walsh.

Linear Reconstruction

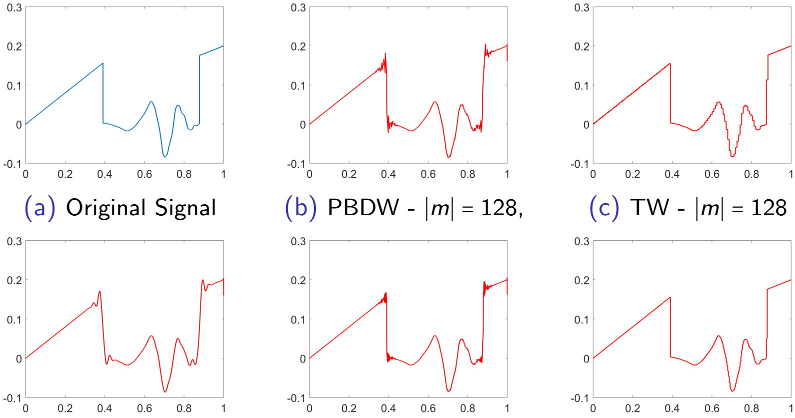

(a) Original Signal (b) PBDW - $|m| = 128$, (c) TW - $|m| = 128$

(d) GS - $|m| = 128$ (e) PBDW - $|m| = 256$ (f) TW - $|m| = 256$

Figure: Linear reconstruction with db8 and $\dim \mathcal{R}_M = 64$.

Fourier Experiment

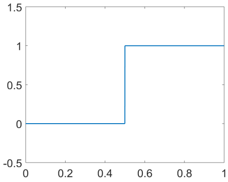

(a) Original Signal

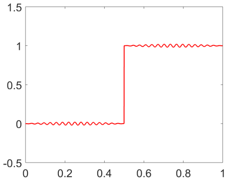

(b) PBDW- $|m| = 64$

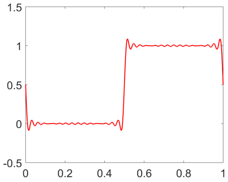

(c) TF - $|m| = 64$

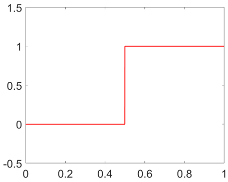

(d) GS - $|m| = 64$

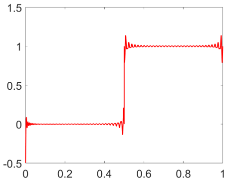

(e) PBDW - $|m| = 256$

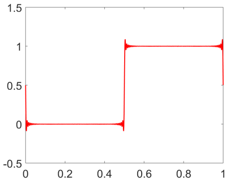

(f) TF - $|m| = 256$

Figure: Fourier measurements with Haar wavelets reconstructoin and $\dim \mathcal{R}_M = 32$

Sampling Pattern

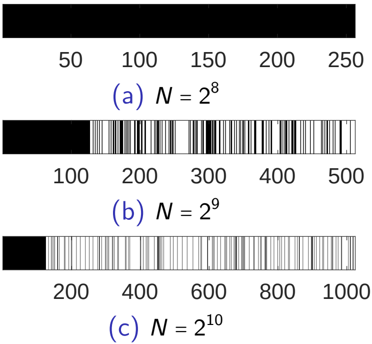

Figure: Sampling pattern with $|m| = 256$, the samples are taken in the black area.

Non-linear Reconstruction

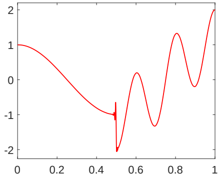

(a) CS with $N = 2^8$

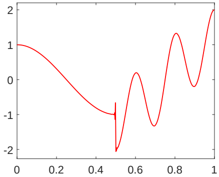

(b) CS with $N = 2^9$

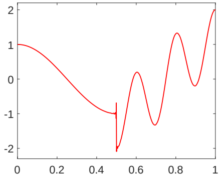

(c) CS with $N = 2^{10}$

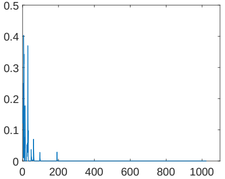

(d) Wav coef $N = 2^8$

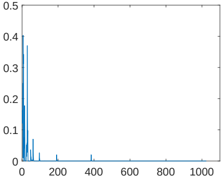

(e) Wav coef $N = 2^9$

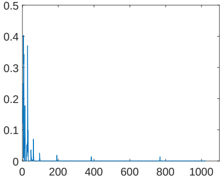

(f) Wav coef $N = 2^{10}$

Figure: Number of samples $|m| = 256$, Wavelet of order $p = 4$

Non-linear Reconstruction

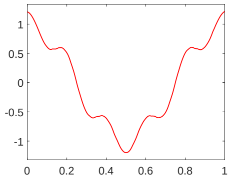

(a) CS

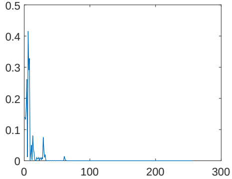

(b) Wav coef

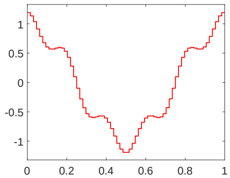

(c) TW - $|m| = 64$

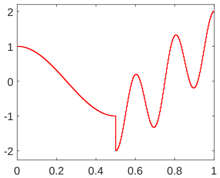

(d) TW - $|m| = 256$

Figure: CS reconstruction with $N = 2^6$, $|m| = 64$ and TW reconstruction.

Impact of Sampling Bandwidth

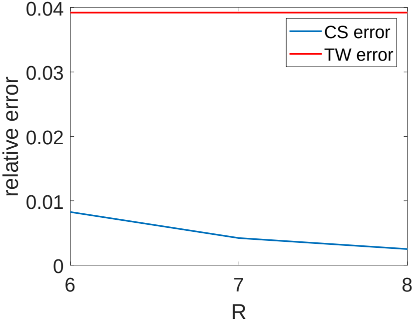

(a) Error plot for reconstruction of f

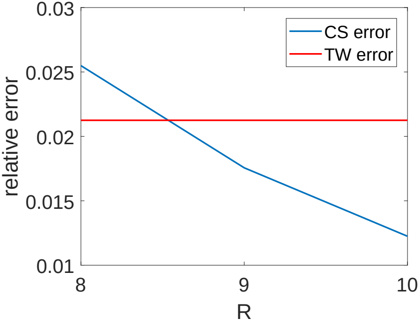

(b) Error plot for reconstruction of g

Figure: CS and truncated Walsh series error values with $|m| = 64$ for f and $|m| = 256$ for g. The x-axis represents the sampling bandwidth $N = 2^R$ and the y-axis the relative error term in the ℓ_2 norm.

Sampling under SSR and Flip Test

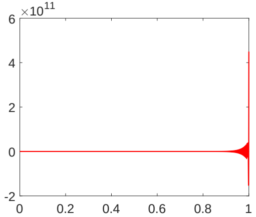

Figure: GS below SSR with $M = 512$ and db8

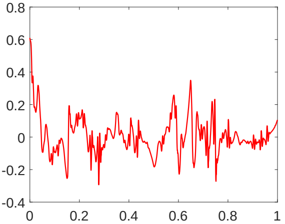

(a) CS reconstruction

(b) Flipped sampling pattern

Figure: Flip test with $N = 2^8$ and $|m| = 64$

Thank you for your attention!

References

B. Adcock and A. C. Hansen.
Generalized sampling and infinite-dimensional compressed sensing.
Foundations of Computational Mathematics, 16(5):1263–1323, 2016.

B. Adcock, A. C. Hansen, C. Poon, and B. Roman.
Breaking the coherence barrier: A new theory for compressed sensing.
In *Forum of Mathematics, Sigma*, volume 5. Cambridge University Press, 2017.

Y. Maday, A. T. Patera, J. D. Penn, and M. Yano.
A parameterized-background data-weak approach to variational data assimilation: formulation, analysis, and application to acoustics.
International Journal for Numerical Methods in Engineering, 102(5):933–965, 2015.

References

A. C. Hansen and L. Thesing.
On the stable sampling rate for binary measurements and wavelet reconstruction.
Appl. Comput. Harmon. Anal., 48(2):630–654, 2020.

L. Thesing and A. C. Hansen.
Non-uniform recovery guarantees for binary measurements and Wavelet reconstruction
to appear.

Related Code

V. Antun.
Spgl1.
https://github.com/vegarant/spgl1, 2017.

V. Antun.
cww - generalized sampling with walsh sampling.
https://github.com/vegarant/cww, 2019.

M. Gataric and C. Poon.
A practical guide to the recovery of wavelet coefficients from fourier measurements.
SIAM J. Sci. Comput., 38(2):A1075–A1099, 2016.

L. Thesing.
infCS.
https://github.com/laurathesing/infCS, 2020.